EUROPEAN ORGANIZATION FOR NUCLEAR RESEARCH

CERN–EP/99–162 Revised

11 November 1999

Upper Limit for the Decay $B^- \to \tau^- \bar{\nu}_\tau$ and Measurement of the $b \to \tau \bar{\nu}_\tau X$ Branching Ratio

DELPHI Collaboration

Abstract

The branching ratio for the leptonic decay of charged B mesons ($B^- \to \tau^- \bar{\nu}_\tau$) has been measured using selected leptonic $\tau^- \to \ell^- \nu_\tau \bar{\nu}_\ell$ and hadronic $\tau \to \nu_\tau X'$ decays in $Z \to b\bar{b}$ decays recorded by DELPHI at LEP1 in 1992-1995. The result, $BR(B^- \to \tau^- \bar{\nu}_\tau) < 1.1 \times 10^{-3}$ at the 90% confidence level, is consistent with Standard Model expectations and puts a constraint on the ratio $\tan\beta/M_{H^\pm} < 0.46$ $(GeV/c^2)^{-1}$ in the framework of models with two Higgs doublets (type II Higgs doublet model). From the missing energy distribution in $Z \to b\bar{b}$ decays without identified leptons, the $b \to \tau \bar{\nu}_\tau X$ branching ratio has been measured in the hadronic channel $\tau \to \nu_\tau X'$. The result, $BR(b \to \tau \bar{\nu}_\tau X) = (2.19 \pm 0.24\ (stat) \pm 0.39\ (syst))\%$, is consistent with the Standard Model prediction and with previous experimental measurements.

(Accepted by Physics Letters B)

P.Abreu[22], W.Adam[52], T.Adye[38], P.Adzic[12], I.Ajinenko[44], Z.Albrecht[18], T.Alderweireld[2], G.D.Alekseev[17], R.Alemany[51], T.Allmendinger[18], P.P.Allport[23], S.Almehed[25], U.Amaldi[9,29], N.Amapane[47], S.Amato[49], E.G.Anassontzis[3], P.Andersson[46], A.Andreazza[9], S.Andringa[22], P.Antilogus[26], W-D.Apel[18], Y.Arnoud[9], B.Åsman[46], J-E.Augustin[26], A.Augustinus[9], P.Baillon[9], P.Bambade[20], F.Barao[22], G.Barbiellini[48], R.Barbier[26], D.Y.Bardin[17], G.Barker[18], A.Baroncelli[40], M.Battaglia[16], M.Baubillier[24], K-H.Becks[54], M.Begalli[6], A.Behrmann[54], P.Beilliere[8], Yu.Belokopytov[9], N.C.Benekos[33], A.C.Benvenuti[5], C.Berat[15], M.Berggren[24], D.Bertrand[2], M.Besancon[41], M.Bigi[47], M.S.Bilenky[17], M-A.Bizouard[20], D.Bloch[10], H.M.Blom[32], M.Bonesini[29], M.Boonekamp[41], P.S.L.Booth[23], A.W.Borgland[4], G.Borisov[20], C.Bosio[43], O.Botner[50], E.Boudinov[32], B.Bouquet[20], C.Bourdarios[20], T.J.V.Bowcock[23], I.Boyko[17], I.Bozovic[12], M.Bozzo[14], M.Bracko[45], P.Branchini[40], R.A.Brenner[50], P.Bruckman[9], J-M.Brunet[8], L.Bugge[34], T.Buran[34], B.Buschbeck[52], P.Buschmann[54], S.Cabrera[51], M.Caccia[28], M.Calvi[29], T.Camporesi[9], V.Canale[39], F.Carena[9], L.Carroll[23], C.Caso[14], M.V.Castillo Gimenez[51], A.Cattai[9], F.R.Cavallo[5], V.Chabaud[9], Ph.Charpentier[9], P.Checchia[37], G.A.Chelkov[17], R.Chierici[47], P.Chliapnikov[9,44], P.Chochula[7], V.Chorowicz[26], J.Chudoba[31], K.Cieslik[19], P.Collins[9], R.Contri[14], E.Cortina[51], G.Cosme[20], F.Cossutti[9], H.B.Crawley[1], D.Crennell[38], S.Crepe[15], G.Crosetti[14], J.Cuevas Maestro[35], S.Czellar[16], M.Davenport[9], W.Da Silva[24], G.Della Ricca[48], P.Delpierre[27], N.Demaria[9], A.De Angelis[48], W.De Boer[18], C.De Clercq[2], B.De Lotto[48], A.De Min[37], L.De Paula[49], H.Dijkstra[9], L.Di Ciaccio[9,39], J.Dolbeau[8], K.Doroba[53], M.Dracos[10], J.Drees[54], M.Dris[33], A.Duperrin[26], J-D.Durand[9], G.Eigen[4], T.Ekelof[50], G.Ekspong[46], M.Ellert[50], M.Elsing[9], J-P.Engel[10], M.Espirito Santo[9], G.Fanourakis[12], D.Fassouliotis[12], J.Fayot[24], M.Feindt[18], A.Ferrer[51], E.Ferrer-Ribas[20], F.Ferro[14], S.Fichet[24], A.Firestone[1], U.Flagmeyer[54], H.Foeth[9], E.Fokitis[33], F.Fontanelli[14], B.Franek[38], A.G.Frodesen[4], R.Fruhwirth[52], F.Fulda-Quenzer[20], J.Fuster[51], A.Galloni[23], D.Gamba[47], S.Gamblin[20], M.Gandelman[49], C.Garcia[51], C.Gaspar[9], M.Gaspar[49], U.Gasparini[37], Ph.Gavillet[9], E.N.Gazis[33], D.Gele[10], T.Geralis[12], L.Gerdyukov[44], N.Ghodbane[26], I.Gil[51], F.Glege[54], R.Gokieli[9,53], B.Golob[9,45], G.Gomez-Ceballos[42], P.Goncalves[22], I.Gonzalez Caballero[42], G.Gopal[38], L.Gorn[1], Yu.Gouz[44], V.Gracco[14], J.Grahl[1], E.Graziani[40], P.Gris[41], G.Grosdidier[20], K.Grzelak[53], J.Guy[38], C.Haag[18], F.Hahn[9], S.Hahn[54], S.Haider[9], A.Hallgren[50], K.Hamacher[54], J.Hansen[34], F.J.Harris[36], V.Hedberg[9,25], S.Heising[18], J.J.Hernandez[51], P.Herquet[2], H.Herr[9], T.L.Hessing[36], J.-M.Heuser[54], E.Higon[51], S-O.Holmgren[46], P.J.Holt[36], S.Hoorelbeke[2], M.Houlden[23], J.Hrubec[52], M.Huber[18], K.Huet[2], G.J.Hughes[23], K.Hultqvist[9,46], J.N.Jackson[23], R.Jacobsson[9], P.Jalocha[19], R.Janik[7], Ch.Jarlskog[25], G.Jarlskog[25], P.Jarry[41], B.Jean-Marie[20], D.Jeans[36], E.K.Johansson[46], P.Jonsson[26], C.Joram[9], P.Juillot[10], L.Jungermann[18], F.Kapusta[24], K.Karafasoulis[12], S.Katsanevas[26], E.C.Katsoufis[33], R.Keranen[18], G.Kernel[45], B.P.Kersevan[45], B.A.Khomenko[17], N.N.Khovanski[17], A.Kiiskinen[16], B.King[23], A.Kinvig[23], N.J.Kjaer[9], O.Klapp[54], H.Klein[9], P.Kluit[32], P.Kokkinias[12], V.Kostioukhine[44], C.Kourkoumelis[3], O.Kouznetsov[17], M.Krammer[52], E.Kriznic[45], J.Krstic[12], Z.Krumstein[17], P.Kubinec[7], J.Kurowska[53], K.Kurvinen[16], J.W.Lamsa[1], D.W.Lane[1], V.Lapin[44], J-P.Laugier[41], R.Lauhakangas[16], G.Leder[52], F.Ledroit[15], V.Lefebure[2], L.Leinonen[46], A.Leisos[12], R.Leitner[31], G.Lenzen[54], V.Lepeltier[20], T.Lesiak[19], M.Lethuillier[41], J.Libby[36], W.Liebig[54], D.Liko[9], A.Lipniacka[9,46], I.Lippi[37], B.Loerstad[25], J.G.Loken[36], J.H.Lopes[49], J.M.Lopez[42], R.Lopez-Fernandez[15], D.Loukas[12], P.Lutz[41], L.Lyons[36], J.MacNaughton[52], J.R.Mahon[6], A.Maio[22], A.Malek[54], T.G.M.Malmgren[46], S.Maltezos[33], V.Malychev[17], F.Mandl[52], J.Marco[42], R.Marco[42], B.Marechal[49], M.Margoni[37], J-C.Marin[9], C.Mariotti[9], A.Markou[12], C.Martinez-Rivero[20], F.Martinez-Vidal[51], S.Marti i Garcia[9], J.Masik[13], N.Mastroyiannopoulos[12], F.Matorras[42], C.Matteuzzi[29], G.Matthiae[39], F.Mazzucato[37], M.Mazzucato[37], M.Mc Cubbin[23], R.Mc Kay[1], R.Mc Nulty[23], G.Mc Pherson[23], C.Meroni[28], W.T.Meyer[1], A.Miagkov[44], E.Migliore[9], L.Mirabito[26], W.A.Mitaroff[52], U.Mjoernmark[25], T.Moa[46], M.Moch[18], R.Moeller[30], K.Moenig[9,11], M.R.Monge[14], D.Moraes[49], X.Moreau[24], P.Morettini[14], G.Morton[36], U.Mueller[54], K.Muenich[54], M.Mulders[32], C.Mulet-Marquis[15], R.Muresan[25], W.J.Murray[38], B.Muryn[19], G.Myatt[36], T.Myklebust[34], F.Naraghi[15], M.Nassiakou[12], F.L.Navarria[5], S.Navas[51], K.Nawrocki[53], P.Negri[29], N.Neufeld[9], R.Nicolaidou[41], B.S.Nielsen[30], P.Niezurawski[53], M.Nikolenko[10,17], V.Nomokonov[16], A.Nygren[25], V.Obraztsov[44], A.G.Olshevski[17], A.Onofre[22], R.Orava[16], G.Orazi[10], K.Osterberg[16], A.Ouraou[41], M.Paganoni[29], S.Paiano[5], R.Pain[24], R.Paiva[22], J.Palacios[36], H.Palka[19], Th.D.Papadopoulou[9,33], L.Pape[9], C.Parkes[9], F.Parodi[14], U.Parzefall[23], A.Passeri[40], O.Passon[54], T.Pavel[25], M.Pegoraro[37], L.Peralta[22], M.Pernicka[52], A.Perrotta[5], C.Petridou[48], A.Petrolini[14], H.T.Phillips[38], F.Pierre[41], M.Pimenta[22], E.Piotto[28], T.Podobnik[45], M.E.Pol[6], G.Polok[19], P.Poropat[48], V.Pozdniakov[17], P.Privitera[39], N.Pukhaeva[17], A.Pullia[29], D.Radojicic[36], S.Ragazzi[29], H.Rahmani[33], J.Rames[13], P.N.Ratoff[21], A.L.Read[34], P.Rebecchi[9], N.G.Redaelli[29], J.Rehn[18], D.Reid[32], R.Reinhardt[54], P.B.Renton[36], L.K.Resvanis[3], F.Richard[20], J.Ridky[13], G.Rinaudo[47], I.Ripp-Baudot[10], O.Rohne[34], A.Romero[47], P.Ronchese[37], E.I.Rosenberg[1], P.Rosinsky[7], P.Roudeau[20], T.Rovelli[5], Ch.Royon[41], V.Ruhlmann-Kleider[41], A.Ruiz[42], H.Saarikko[16], Y.Sacquin[41], A.Sadovsky[17], G.Sajot[15], J.Salt[51], D.Sampsonidis[12], M.Sannino[14], Ph.Schwemling[24], B.Schwering[54], U.Schwickerath[18], F.Scuri[48], P.Seager[21], Y.Sedykh[17], A.M.Segar[36], N.Seibert[18], R.Sekulin[38], R.C.Shellard[6], M.Siebel[54], L.Simard[41], F.Simonetto[37], A.N.Sisakian[17], G.Smadja[26], N.Smirnov[44], O.Smirnova[25], G.R.Smith[38], A.Sokolov[44], A.Sopczak[18], R.Sosnowski[53], T.Spassov[22], E.Spiriti[40], S.Squarcia[14], C.Stanescu[40], S.Stanic[45], M.Stanitzki[18], K.Stevenson[36], A.Stocchi[20], J.Strauss[52], R.Strub[10], B.Stugu[4], M.Szczekowski[53], M.Szeptycka[53], T.Tabarelli[29], A.Taffard[23], F.Tegenfeldt[50], F.Terranova[29], J.Thomas[36], J.Timmermans[32], N.Tinti[5], L.G.Tkatchev[17], M.Tobin[23], S.Todorova[9], A.Tomaradze[2], B.Tome[22], A.Tonazzo[9], L.Tortora[40], P.Tortosa[51], G.Transtromer[25], D.Treille[9], G.Tristram[8], M.Trochimczuk[53], C.Troncon[28],

M-L.Turluer[41], I.A.Tyapkin[17], P.Tyapkin[25], S.Tzamarias[12], O.Ullaland[9], V.Uvarov[44], G.Valenti[9,5], E.Vallazza[48], P.Van Dam[32], W.Van den Boeck[2], W.K.Van Doninck[2], J.Van Eldik[9,32], A.Van Lysebetten[2], N.van Remortel[2], I.Van Vulpen[32], G.Vegni[28], L.Ventura[37], W.Venus[38,9], F.Verbeure[2], P.Verdier[26], M.Verlato[37], L.S.Vertogradov[17], V.Verzi[28], D.Vilanova[41], L.Vitale[48], E.Vlasov[44], A.S.Vodopyanov[17], G.Voulgaris[3], V.Vrba[13], H.Wahlen[54], C.Walck[46], A.J.Washbrook[23], C.Weiser[9], D.Wicke[54], J.H.Wickens[2], G.R.Wilkinson[36], M.Winter[10], M.Witek[19], G.Wolf[9], J.Yi[1], O.Yushchenko[44], A.Zalewska[19], P.Zalewski[53], D.Zavrtanik[45], E.Zevgolatakos[12], N.I.Zimin[17,25], A.Zintchenko[17], Ph.Zoller[10], G.C.Zucchelli[46], G.Zumerle[37]

[1] Department of Physics and Astronomy, Iowa State University, Ames IA 50011-3160, USA
[2] Physics Department, Univ. Instelling Antwerpen, Universiteitsplein 1, B-2610 Antwerpen, Belgium
and IIHE, ULB-VUB, Pleinlaan 2, B-1050 Brussels, Belgium
and Faculté des Sciences, Univ. de l'Etat Mons, Av. Maistriau 19, B-7000 Mons, Belgium
[3] Physics Laboratory, University of Athens, Solonos Str. 104, GR-10680 Athens, Greece
[4] Department of Physics, University of Bergen, Allégaten 55, NO-5007 Bergen, Norway
[5] Dipartimento di Fisica, Università di Bologna and INFN, Via Irnerio 46, IT-40126 Bologna, Italy
[6] Centro Brasileiro de Pesquisas Físicas, rua Xavier Sigaud 150, BR-22290 Rio de Janeiro, Brazil
and Depto. de Física, Pont. Univ. Católica, C.P. 38071 BR-22453 Rio de Janeiro, Brazil
and Inst. de Física, Univ. Estadual do Rio de Janeiro, rua São Francisco Xavier 524, Rio de Janeiro, Brazil
[7] Comenius University, Faculty of Mathematics and Physics, Mlynska Dolina, SK-84215 Bratislava, Slovakia
[8] Collège de France, Lab. de Physique Corpusculaire, IN2P3-CNRS, FR-75231 Paris Cedex 05, France
[9] CERN, CH-1211 Geneva 23, Switzerland
[10] Institut de Recherches Subatomiques, IN2P3 - CNRS/ULP - BP20, FR-67037 Strasbourg Cedex, France
[11] Now at DESY-Zeuthen, Platanenallee 6, D-15735 Zeuthen, Germany
[12] Institute of Nuclear Physics, N.C.S.R. Demokritos, P.O. Box 60228, GR-15310 Athens, Greece
[13] FZU, Inst. of Phys. of the C.A.S. High Energy Physics Division, Na Slovance 2, CZ-180 40, Praha 8, Czech Republic
[14] Dipartimento di Fisica, Università di Genova and INFN, Via Dodecaneso 33, IT-16146 Genova, Italy
[15] Institut des Sciences Nucléaires, IN2P3-CNRS, Université de Grenoble 1, FR-38026 Grenoble Cedex, France
[16] Helsinki Institute of Physics, HIP, P.O. Box 9, FI-00014 Helsinki, Finland
[17] Joint Institute for Nuclear Research, Dubna, Head Post Office, P.O. Box 79, RU-101 000 Moscow, Russian Federation
[18] Institut für Experimentelle Kernphysik, Universität Karlsruhe, Postfach 6980, DE-76128 Karlsruhe, Germany
[19] Institute of Nuclear Physics and University of Mining and Metalurgy, Ul. Kawiory 26a, PL-30055 Krakow, Poland
[20] Université de Paris-Sud, Lab. de l'Accélérateur Linéaire, IN2P3-CNRS, Bât. 200, FR-91405 Orsay Cedex, France
[21] School of Physics and Chemistry, University of Lancaster, Lancaster LA1 4YB, UK
[22] LIP, IST, FCUL - Av. Elias Garcia, 14-1^{o}, PT-1000 Lisboa Codex, Portugal
[23] Department of Physics, University of Liverpool, P.O. Box 147, Liverpool L69 3BX, UK
[24] LPNHE, IN2P3-CNRS, Univ. Paris VI et VII, Tour 33 (RdC), 4 place Jussieu, FR-75252 Paris Cedex 05, France
[25] Department of Physics, University of Lund, Sölvegatan 14, SE-223 63 Lund, Sweden
[26] Université Claude Bernard de Lyon, IPNL, IN2P3-CNRS, FR-69622 Villeurbanne Cedex, France
[27] Univ. d'Aix - Marseille II - CPP, IN2P3-CNRS, FR-13288 Marseille Cedex 09, France
[28] Dipartimento di Fisica, Università di Milano and INFN-MILANO, Via Celoria 16, IT-20133 Milan, Italy
[29] Dipartimento di Fisica, Univ. di Milano-Bicocca and INFN-MILANO, Piazza delle Scienze 2, IT-20126 Milan, Italy
[30] Niels Bohr Institute, Blegdamsvej 17, DK-2100 Copenhagen Ø, Denmark
[31] IPNP of MFF, Charles Univ., Areal MFF, V Holesovickach 2, CZ-180 00, Praha 8, Czech Republic
[32] NIKHEF, Postbus 41882, NL-1009 DB Amsterdam, The Netherlands
[33] National Technical University, Physics Department, Zografou Campus, GR-15773 Athens, Greece
[34] Physics Department, University of Oslo, Blindern, NO-1000 Oslo 3, Norway
[35] Dpto. Fisica, Univ. Oviedo, Avda. Calvo Sotelo s/n, ES-33007 Oviedo, Spain
[36] Department of Physics, University of Oxford, Keble Road, Oxford OX1 3RH, UK
[37] Dipartimento di Fisica, Università di Padova and INFN, Via Marzolo 8, IT-35131 Padua, Italy
[38] Rutherford Appleton Laboratory, Chilton, Didcot OX11 OQX, UK
[39] Dipartimento di Fisica, Università di Roma II and INFN, Tor Vergata, IT-00173 Rome, Italy
[40] Dipartimento di Fisica, Università di Roma III and INFN, Via della Vasca Navale 84, IT-00146 Rome, Italy
[41] DAPNIA/Service de Physique des Particules, CEA-Saclay, FR-91191 Gif-sur-Yvette Cedex, France
[42] Instituto de Fisica de Cantabria (CSIC-UC), Avda. los Castros s/n, ES-39006 Santander, Spain
[43] Dipartimento di Fisica, Università degli Studi di Roma La Sapienza, Piazzale Aldo Moro 2, IT-00185 Rome, Italy
[44] Inst. for High Energy Physics, Serpukov P.O. Box 35, Protvino, (Moscow Region), Russian Federation
[45] J. Stefan Institute, Jamova 39, SI-1000 Ljubljana, Slovenia and Laboratory for Astroparticle Physics,
Nova Gorica Polytechnic, Kostanjeviska 16a, SI-5000 Nova Gorica, Slovenia,
and Department of Physics, University of Ljubljana, SI-1000 Ljubljana, Slovenia
[46] Fysikum, Stockholm University, Box 6730, SE-113 85 Stockholm, Sweden
[47] Dipartimento di Fisica Sperimentale, Università di Torino and INFN, Via P. Giuria 1, IT-10125 Turin, Italy
[48] Dipartimento di Fisica, Università di Trieste and INFN, Via A. Valerio 2, IT-34127 Trieste, Italy
and Istituto di Fisica, Università di Udine, IT-33100 Udine, Italy
[49] Univ. Federal do Rio de Janeiro, C.P. 68528 Cidade Univ., Ilha do Fundão BR-21945-970 Rio de Janeiro, Brazil
[50] Department of Radiation Sciences, University of Uppsala, P.O. Box 535, SE-751 21 Uppsala, Sweden
[51] IFIC, Valencia-CSIC, and D.F.A.M.N., U. de Valencia, Avda. Dr. Moliner 50, ES-46100 Burjassot (Valencia), Spain
[52] Institut für Hochenergiephysik, Österr. Akad. d. Wissensch., Nikolsdorfergasse 18, AT-1050 Vienna, Austria
[53] Inst. Nuclear Studies and University of Warsaw, Ul. Hoza 69, PL-00681 Warsaw, Poland
[54] Fachbereich Physik, University of Wuppertal, Postfach 100 127, DE-42097 Wuppertal, Germany

1 Introduction

The purely leptonic decay $B^- \to \tau^- \bar{\nu}_\tau$ [1] is of particular interest to test for deviations from the Standard Model. In the Standard Model the heavy b quark annihilates with the light $\bar{u}$ antiquark forming a virtual W^- boson which decays leptonically. The width of the decay $B^- \to \tau^- \bar{\nu}_\tau$ is predicted to be

$$, ^{SM}(B^- \to \tau^- \bar{\nu}_\tau) = \frac{G_F^2 f_B^2 |V_{ub}|^2}{8\pi} m_B^3 \left(\frac{m_\tau}{m_B}\right)^2 \left(1 - \frac{m_\tau^2}{m_B^2}\right)^2 \quad (1)$$

where G_F is the Fermi coupling constant, $|V_{ub}|$ is the modulus of the CKM matrix element, f_B is the B decay constant, m_B is the mass of the B meson, and m_τ is the mass of the τ lepton. The expected branching fraction is [1]

$$BR^{SM}(B^- \to \tau^- \bar{\nu}_\tau) = 6 \times 10^{-5} \cdot (f_B/190\ \text{MeV})^2 \cdot (|V_{ub}|/0.003)^2.$$

Because of helicity conservation, the purely leptonic decay widths are proportional to the square of the lepton mass. The branching fractions into electron or muon are therefore expected to be very small, $BR^{SM}(B^- \to \mu^- \bar{\nu}_\mu) \simeq 3 \times 10^{-7}$ and $BR^{SM}(B^- \to e^- \bar{\nu}_e) \simeq 6 \times 10^{-12}$, and therefore to be unobservable at LEP.

Because of the larger lepton mass, the partial decay width for the decay $B^- \to \tau^- \bar{\nu}_\tau$ is not only much larger, but is also much more sensitive to Higgs-sector physics beyond the Standard Model. In models with two Higgs doublets (the so called Type II Higgs models), the decay width can be significantly enhanced by the contribution of charged Higgs bosons. In such models the branching fraction becomes [2]

$$BR(B^- \to \tau^- \bar{\nu}_\tau) = BR^{SM}(B^- \to \tau^- \bar{\nu}_\tau) \cdot \left[\left(\frac{m_{B^-}}{m_{H^\pm}}\right)^2 \tan^2\beta - 1\right]^2 \quad (2)$$

where $m_{H^\pm}$ is the charged Higgs boson mass and $\tan\beta$ is the ratio of the vacuum expectation values of the two Higgs doublets.

However, no evidence for an enhancement relative to the Standard Model prediction was observed in previous experimental studies by CLEO [3], ALEPH [4] and L3 [5]. These studies constrain the parameters of models with two Higgs doublets. The best upper limit is from L3: $BR(B^- \to \tau^- \bar{\nu}_\tau) < 5.7 \times 10^{-4}$ at 90% confidence level.

Complications in interpreting such a limit arise from the large current uncertainty on $f_B^2 |V_{ub}|^2$ in (1), and also from the fact that the production of B_c mesons decaying leptonically can give a substantial contribution to the $\tau\bar{\nu}_\tau$ final state, because for B_c mesons the coupling of the virtual $W^\pm$ involves the CKM matrix element V_{cb} instead of V_{ub}. The B_c meson was recently observed by the CDF collaboration [6]. Its measured mass and lifetime agree with current expectations. Within an uncertainty of a factor two, the relative fraction of $\tau\bar{\nu}_\tau$ final states coming from B_c and B_u production at LEP1 is given by

$$\frac{N_{B_c}}{N_{B_u}} = 1.2\ \frac{f(b \to B_c)}{10^{-3}} \quad (3)$$

where $f(b \to B_c)$, the inclusive probability that a b quark hadronizes into a B_c meson, is expected to be between 0.02% and 0.1% [7].

The other decay studied here, the decay $b \to \tau\bar{\nu}_\tau X$ where X stands for all the other particles produced, provides another test of the Standard Model. The Standard Model

[1] In this paper, corresponding statements for charge conjugate states are generally implied unless explicitly stated otherwise.

predicts a $b \to \tau\bar{\nu}_\tau X$ branching fraction of $(2.30 \pm 0.25)\%$ in the framework of the Heavy Quark Effective Theory (HQET) [8,9]. Extensions of the Standard Model with two Higgs doublets also predict an enhancement of this decay [10,11], because it too can be mediated by H^- as well as by W^- exchange. Therefore, an experimental measurement of this branching fraction also constrains the ratio $\tan\beta/m_{H^\pm}$. Furthermore, the particular complications mentioned above concerning the interpretation of the $B^- \to \tau^-\bar{\nu}_\tau$ decay rate do not arise in this case.

The decay $b \to \tau\bar{\nu}_\tau X$ is suppressed by phase space compared with the other semileptonic b decays. However, it is more sensitive to the contribution from $H^\pm$ exchange, because this contribution is proportional to $(m_{\rm lepton}/m_{H^\pm})^2$. Previous experimental measurements of BR($b \to \tau\bar{\nu}_\tau X$), by ALEPH [4], L3 [12] and OPAL [13], are consistent with the Standard Model.

This paper presents an upper limit on the exclusive branching fraction $B^- \to \tau^-\bar{\nu}_\tau$ and a measurement of the inclusive branching fraction $b \to \tau\bar{\nu}_\tau X$.

2 Sample selection

About 3.5 million hadronic decays of the Z were collected with the DELPHI detector [14,15] at LEP1 in 1992-1995. For comparison with these data, about 7 million simulated Z decays to hadrons ("$q\bar{q}$" events) from the JETSET Parton Shower model [16] with the Peterson parametrization [17] for the fragmentation of b and c quarks were processed with full simulation of the DELPHI detector, together with a further 10000 such events with a B^- meson decaying into $\tau\bar{\nu}_\tau$.

For each event, the position of the e^+e^- interaction (or "primary vertex") was reconstructed from the charged particle tracks and the mean beam spot. In the 1994 and 1995 data, this was determined with a precision of about 40 μm in the horizontal direction, and about 10 μm in the vertical direction. The uncertainties were about 50% larger in 1992 and 1993. Charged particle tracks were accepted provided their impact parameters with respect to the e^+e^- interaction were less than 2 cm both along the beam and in the transverse plane.

The initial event selections applied in all the analyses presented here required:

a) more than seven charged particles with a total energy (assuming them to be pions) above 15 GeV (to select hadronic events);
b) all subdetectors needed for the analysis fully operational;
c) thrust of the event above 0.85 (to select a two jet topology);
d) angle θ_t between the thrust axis and the beam satisfying $0.1 < |\cos\theta_t| < 0.7$ (to match the vertex detector acceptance);
e) the probability, P_E, that all charged particle tracks in the event originated from a common primary vertex [18] satisfying P_E below 0.01; this selected $Z^0 \to b\bar{b}$ events with an efficiency of 72% and a purity of 75%.

The analyses using τ hadronic decays required efficient rejection of electrons and muons. Hence these analyses used "loose" criteria to identify electrons, with an efficiency of 80% and a hadron misidentification probability of about 1.6% [15], and "very loose" criteria for muons (requiring just one hit in the muon chambers) with an identification efficiency of 96% and a hadron misidentification probability of about 5.4% [15]. In both cases the momentum of the lepton was required to be above 2 GeV/c.

The analyses using τ leptonic decays required clean samples. Hence these analyses used "tight" lepton identification criteria [15]. For electrons (muons), these gave an efficiency of 45% (70%) and a hadron misidentification probability of 0.2% (0.45%).

3 The energy reconstruction

Each selected event was divided into two hemispheres by the plane perpendicular to the thrust axis. In each hemisphere the missing energy, $E_{\rm miss}$, was calculated from the expression

$$E_{\rm miss} = E_{\rm true} - E_{\rm vis} \tag{4}$$

where $E_{\rm true} = E_{\rm beam} + (M^2_{\rm same} - M^2_{\rm oppo})/(4E_{\rm beam})$ is a hemisphere energy calculated from the beam energy, $E_{\rm beam}$, using 4-momentum conservation and the invariant mass of all reconstructed particles in the hemisphere considered, $M_{\rm same}$, and in the opposite hemisphere, $M_{\rm oppo}$. The visible energy, $E_{\rm vis}$, in the hemisphere considered is

$$E_{\rm vis} = E_{\rm ch} + E_\gamma + E_{\rm oth} + E_{\rm HCAL} \tag{5}$$

where, in that hemisphere,

- $E_{\rm ch}$ is the energy sum of the selected charged particles. It also includes the energy sum of V^0 candidates (long-lived neutral particles decaying into two oppositely-charged particles) identified with a "loose" criterion [15].
- E_γ is the energy sum of photons and π^0's. About 7% of the photons convert in front of the TPC, creating e^+e^- pairs which can be reconstructed. Photon showers in the electromagnetic calorimeters (HPC, FEMC) are identified through their characteristic longitudinal and transverse shower profiles. A π^0 is reconstructed either by pairing photons (converted before the TPC or detected in the electromagnetic calorimeters), or by analysing the energy deposit of an isolated electromagnetic shower [15].
- $E_{\rm oth}$ is the energy sum of electromagnetic calorimeter clusters that are not from photons or π^0's and are not associated to charged particle tracks.
- $E_{\rm HCAL}$ is the energy sum of hadron calorimeter clusters not associated to charged particle tracks.

In these energy computations, the pion mass was assumed for charged particles and the photon mass for neutral particles.

4 Upper limit for the decay $B^- \to \tau^- \bar{\nu}_\tau$

The decay $B^- \to \tau^- \bar{\nu}_\tau$ was studied with one-prong decay modes of the τ lepton in:

1) the τ leptonic decay channel (with branching fraction $\simeq$ 35% [22]) when the τ^- decays into $\ell^- \nu_\tau \bar{\nu}_\ell$, where ℓ^- is either an electron or a muon,
2) the τ hadronic decay channel (with branching fraction $\simeq$ 50% [22]) when the τ^- decays to $h^- \nu_\tau X$, where h^- is a charged hadron and X is a system of neutral hadrons (mostly π^0's).

4.1 The τ leptonic decay channel

In the leptonic channel, the charged lepton ℓ (μ or e) was selected using tight criteria (see Section 2). The lepton had to be in the hemisphere with the larger missing energy: this selected 90% of the simulated $B^- \to \tau^- \bar{\nu}_\tau$ decays with $\tau^- \to \ell^- \nu_\tau \bar{\nu}_\ell$.

The impact parameter of each track is defined here as the shortest distance between the track and the reconstructed primary vertex in the plane transverse to the beam direction. The impact parameter was signed positive if the angle between its direction and the direction of the jet to which the track belonged was smaller than 90° ("lifetime sign") [15]. The impact parameter of the lepton had to be positive and four times larger than its measured error, i.e. above $+4\sigma$.

In the τ^- rest frame, due to helicity conservation, the ℓ^- is emitted preferentially in a direction opposite to the flight direction of the τ^-. As a consequence, in the laboratory frame the lepton energy distributions for the signal and the background are similar, as shown in Figure 1, and the lepton energy cannot be used as a discriminating variable (here and below the background events are simulated hadronic Z events to which the same selection criteria are applied).

The background from heavy flavour semileptonic decays can be substantially reduced with a constrained kinematic fit. This is because a b-hadron takes a large fraction of the jet energy and in a $B^- \to \tau^- \bar{\nu}_\tau$ decay the lepton ℓ is its only detectable product, while background events from semileptonic decays give additional B decay products. For the signal, the energy and momentum of the B meson can be reconstructed from energy-momentum conservation applied to the whole event:

$$\overrightarrow{P_{\rm B}} = -\sum_{i \neq \ell} \overrightarrow{P_i}, \qquad E_{\rm B} = \sqrt{s} - \sum_{i \neq \ell} E_i \tag{6}$$

where the summation is performed over all detected particles in the event except the lepton ℓ. The energies of all reconstructed particles ($E_i^{\rm fit}$) are then varied in the kinematic fit, in order to minimize their deviations relative to the experimentally measured values ($E_i^{\rm meas}$):

$$\chi^2 = \sum_{i \neq \ell} \frac{(E_i^{\rm fit} - E_i^{\rm meas})^2}{\sigma^2_{E_i^{\rm meas}}} \tag{7}$$

with the constraint $E_{\rm B}^2 - \overrightarrow{P_{\rm B}}^2 = M_{\rm B}^2$.

The fitted value of $E_{\rm B}$ was required to exceed 37 GeV (see Figure 1). All tracks in the lepton hemisphere except the lepton were required to have an impact parameter of less than 3σ with respect to the primary vertex, and a momentum, $P_{\rm max}$, less than 5 GeV/c. The multiplicity of charged particles in the selected hemisphere had to be less than 6. Since the lepton to be selected is from two successive leptonic decays, it tends to be isolated from other particles. Hence the sum of the energies, $E_{\rm cone}$, of all particles within a cone with half opening angle of 0.5 radian around the lepton direction was required to be below 12 GeV, and their invariant mass, $M_{\rm cone}$, had to be below 3 GeV/c^2. Figure 1 shows the distributions of these quantities for signal and background, and the cuts chosen.

These selections gave a background rejection factor of 7400 ± 1800, and a selection efficiency of $B^- \to \tau^- \bar{\nu}_\tau$ leptonic events of $(6.5 \pm 1.3)\%$, with respect to the number of events after the kinematic fit. They selected 3 events in real data, while 5 were predicted by the $q\bar{q}$ background simulation.

4.2 The τ hadronic decay channel

In the hadronic channel, only hemispheres with no $e^{\pm}$ or $\mu^{\pm}$ were selected. To reject semileptonic decays efficiently, the lepton identification criteria were loosened as indicated in Section 2. As in the leptonic channel analysis, the candidate τ decay product, this time a hadron h, had to be in the hemisphere with the larger missing energy (this requirement accepted 88% of the signal events), and its impact parameter relative to the primary vertex had to exceed $+4\sigma$. The energy $E_{\rm h}$ of the most energetic such candidate had to be below 10 GeV.

Since most of the hadronic decays are of the type $\tau^- \to {\rm h}^-\nu_\tau n\pi^0$ (with $n \geq 1$), identified π^0's and γ's were selected inside a cone of half-opening angle equal to 0.5 radian around the direction of h. The energy and momentum of the B meson were reconstructed as

$$\overrightarrow{P_{\rm B}} = - \sum_{i\neq {\rm h},\pi^0,\gamma \text{ in cone}} \overrightarrow{P_i}\ , \qquad E_{\rm B} = \sqrt{s} - \sum_{i\neq {\rm h},\pi^0,\gamma \text{ in cone}} E_i, \tag{8}$$

where the summation is performed over all detected particles of the event, except the charged hadron h and possible π^0's and γ's detected inside the cone, which were assumed to be additional τ decay products.

As in the leptonic channel, the energies of these particles were then fitted with the constraint $E_{\rm B}^2 - \overrightarrow{P_{\rm B}}^2 = M_{\rm B}^2$, and E_B was required to exceed 37 GeV (see Figure 2). The other charged particles in the hemisphere were selected if their impact parameter relative to the primary vertex was below 4σ and their momentum below 2 GeV/c. Their multiplicity had to be less than eight. The total neutral energy in the cone was required to be below 4 GeV, and the total energy and invariant mass of the whole system of particles inside the cone had to be below 7 GeV and 2 GeV/c^2, respectively (see Figure 2).

These selections gave a background rejection factor of 7400 ± 1100, and a selection efficiency of $B^- \to \tau^-\bar{\nu}_\tau$ hadronic events of $(3.2 \pm 0.5)\%$, with respect to the number of events after the kinematic fit. They selected 17 events in real data, while 20 were predicted by the $q\bar{q}$ background simulation.

4.3 Combined result

In both channels, leptonic and hadronic, no evidence was observed for an excess of events in data over the background estimate. From the expected and observed numbers quoted above, the Bayesian upper limit (for two combined channels with background and known relative rates [20]) on the number of $B^- \to \tau^-\bar{\nu}_\tau$ decays was 3.5 at 90% confidence level.

The main sources of systematic uncertainties were included in the limit evaluation, including uncertainties in the $\tau^- \to \ell^-\nu_\tau\bar{\nu}_\ell$ and $\tau^- \to \nu_\tau {\rm X}$ branching fractions, the b-tagging efficiency, the lepton selection efficiency, and the hadron misidentification rate. The largest contribution was from the evaluation of the probability for b quarks to hadronize into charged B^- mesons, 0.389 ± 0.013 [22]. However, the systematic uncertainties had only a small effect.

Assuming no B_c contribution, the above upper limit on the number of events gave

$$\mathrm{BR}(B^- \to \tau^-\bar{\nu}_\tau) < 1.1 \times 10^{-3} \tag{9}$$

at 90% confidence level.

5 Measurement of the $b \to \tau\bar{\nu}_\tau X$ branching fraction

The main signature of the decay chain $b \to \tau\bar{\nu}_\tau X$ with $\tau \to \nu_\tau X'$ is a large missing energy due to the production of two or three neutrinos. The main backgrounds are from semileptonic b and c decays into e or μ with high-energy neutrinos, and from hadronic events with large missing energy due to the finite resolution of the detector.

To reduce these backgrounds, an enriched sample of $b \to \tau\bar{\nu}_\tau X$ candidates was selected in two steps. First, as already mentioned, a sample enriched in $Z \to b\bar{b}$ events was obtained by requiring $P_E \leq 0.01$. Then, in order to reject heavy flavour semileptonic decays efficiently, leptons were identified with the loose criterion for electrons and the very loose criterion for muons as in Section 4.2, and hemispheres with such a lepton were rejected. The τ lepton therefore had to decay hadronically: $\tau \to \nu_\tau X'$, where X' are hadrons. In addition, since this analysis is more sensitive to detector inefficiencies than the previous ones, criterion d) of Section 2 on the thrust axis polar direction θ_t was tightened to $0.2 < |\cos\theta_t| < 0.6$.

5.1 Energy correction procedure

In order to improve the agreement of the energy measurement between the backgrounds in the real data (RD_b) and in the simulation (MC_b), the following correction procedure was used. First, a detailed comparison with the corresponding real data was used to determine a multiplicity-dependent correction to the distribution of visible energy, E_{vis}, in a simulated sample enriched with light quark pair ($u\bar{u}$, $d\bar{d}$, $s\bar{s}$) events. Then the same correction was applied to the MC_b sample.

To obtain enriched samples of light quark events in real data (RD_{uds}) and simulation (MC_{uds}), the selection criteria mentioned in Section 2 were used, except that criterion e) was changed to:

e′) $0.6 < P_E < 1.0$, which corresponds to an efficiency of 41% and a purity of 91% for light quark pair events.

The corrected visible energy in the simulated sample, already defined in Section 3, was then parametrized as

$$E_{vis}^{MC} = c_0 + c_1 E_{ch} + c_2 E_\gamma + c_3 E_{oth} + c_4 E_{HCAL} \tag{10}$$

where the coefficients c_j $(j = 0, ..., 4)$ depended on the multiplicity of charged particles in the hemisphere considered, and were determined by minimizing

$$\chi^2 = \sum_{k=1}^{5} \frac{(M_k^{RD_{uds}} - M_k^{MC_{uds}})^2}{D_k^{RD_{uds}}} \tag{11}$$

separately for each charged particle multiplicity in the hemisphere. In this expression, $M_1^{RD_{uds}}$ and $M_1^{MC_{uds}}$ are the mean visible energies in real data and simulated events respectively, $M_k^{RD_{uds}}$ and $M_k^{MC_{uds}}$ $(k = 2, ..., 5)$ are central moments of order k of the E_{vis} distribution in real data and simulated events respectively, and $D_k^{RD_{uds}}$ is the variance of the $M_k^{RD_{uds}}$ distribution. After this correction to E_{vis} in the simulated sample, the real and simulated E_{miss} distributions agreed (Figure 3).

The fragmentation and hadronization of b-quarks differ from those of light quarks. However it was checked in the simulation that, for the same charged multiplicity, the energy distributions of E_{ch}, E_γ, E_{oth} and E_{HCAL} are very similar in $b\bar{b}$ and light quark pair events. The same coefficients c_j were therefore applied to the MC_b sample, and corrected values E_{vis}^{MC} were obtained.

5.2 Result

A sub-sample of $b \to \tau\bar{\nu}_\tau X$ events, MC_b^τ, was isolated from the sample MC_b by requiring that the Z decayed into a $b\bar{b}$ pair and that the b decay products contained a τ lepton in one hemisphere. The complementary sub-sample, MC_b^{bkg}, contained all other possible decay modes and corresponded to the background simulation; it was subdivided into the semileptonic background, $MC_b^{\ell X}$, and the residual background, $MC_b^{res.bkg}$.

Figure 4 shows the hemisphere missing energy distributions of the RD_b sample, which was fitted as follows. The normalization of the $MC_b^{\ell X}$ sample was fixed by the known branching fractions and the estimated selection efficiencies (see Section 5.3). The normalizations of the MC_b^τ and $MC_b^{res.bkg}$ samples were treated as free parameters. The overall $MC_b^\tau + MC_b^{bkg}$ sample was normalized to the number of events in the RD_b sample.

The fit used the missing energy range from -5 GeV to 30 GeV where the main part of the signal is concentrated. The branching fraction of $b \to \tau\bar{\nu}_\tau X$ was measured to be

$$BR(b \to \tau\bar{\nu}_\tau X) = (2.19 \pm 0.24\ (stat))\% \ .$$

Figure 5 shows the difference between the distributions of events in the RD_b and MC_b^{bkg} sample. Its shape is consistent with that expected from the MC_b^τ component (shaded area).

5.3 Evaluation of systematic uncertainties

Table 1 summarizes the systematic uncertainties on the measured branching fraction.

Absolute variations of the parameters	$\Delta(b \to \tau\bar{\nu}_\tau X)$ (%)
$BR(b \to \ell) = (10.73 \pm 0.18)\%$	0.003
$BR(b \to c \to \bar{\ell}) = (8.3 \pm 0.4)\%$	0.045
$BR(b \to \bar{c} \to \ell) = (1.6 \pm 0.4)\%$	0.041
$BR(c \to \bar{\ell}) = (9.6 \pm 0.5)\%$	0.035
modelling of all the above decays	0.039
μ identification efficiency ($\pm 1.2\%$)	0.012
e identification efficiency ($\pm 3\%$)	0.025
hadron $\to \mu$ misident. prob. ($\pm 2.0\%$)	0.098
hadron $\to$ e misident. prob. ($\pm 0.3\%$)	0.012
b-tagging purity ($\pm 2\%$)	0.039
$BR(b \to D_s) = (18 \pm 5)\%$	0.037
$BR(D_s \to \tau\nu) = (7 \pm 4)\%$	0.068
$< x_b >= 0.702 \pm 0.008$	0.210
$< x_c >= 0.484 \pm 0.008$	0.030
shape of background E_{miss} distribution	0.250
E_{miss} range fitted	0.150
Total Systematic Uncertainty	0.393

Table 1: Systematic uncertainties on $BR(b \to \tau\bar{\nu}_\tau X\ )$

The main physics background comes from the semileptonic decays of b and c quarks into e and μ that were not identified. The uncertainty on the branching fractions of these decays contributes to the systematic uncertainty. Varying the branching fraction $BR(b \to \ell) = (10.73 \pm 0.18)\%$ [22] by one standard deviation contributed an absolute uncertainty on $BR(b \to \tau\bar{\nu}_\tau X\ )$ of $\pm 0.003\%$. Similarly, varying $BR(b \to c \to \overline{\ell}) = (8.3 \pm 0.4)\%$ [22]

contributed $\pm 0.045\%$, varying $\mathrm{BR}(\mathrm{b} \to \overline{\mathrm{c}} \to \ell) = (1.6 \pm 0.4)\%$ [23] contributed $\pm 0.041\%$, and varying $\mathrm{BR}(\mathrm{c} \to \overline{\ell}) = (9.6 \pm 0.5)\%$ [24], contributed $\pm 0.035\%$.

Most of the background from semileptonic decays of b and c quarks was due to leptons that could not be identified because their momenta were below 2 GeV/c. The uncertainties in the modelling of the above semileptonic decays, and the consequent uncertainties on the fractions of leptons produced with momenta below 2 GeV/c (see Table 7 of reference [24]), contributed a further uncertainty of $\pm 0.039\%$.

A possible difference between data and simulation on the lepton identification had also to be taken into account. The uncertainty of $\pm 1.2\%$ ($\pm 3\%$) on the μ (e) identification efficiency [15] contributed an uncertainty of $\pm 0.012\%$ ($\pm 0.025\%$). Similarly, the uncertainty on the hadron misidentification probability, $\pm 2\%$ ($\pm 0.3\%$) for μ (e) [15], contributed $\pm 0.098\%$ ($\pm 0.012\%$).

The difference in the b-tagging purity for data and simulation is also relevant, because the fraction of real $\mathrm{b\overline{b}}$ events in the selected sample directly influences the value of the measured branching fraction. This difference, estimated to be approximately $\pm 2\%$, contributed an uncertainty of $\pm 0.039\%$.

The only significant background from τ leptons comes from the decay $\mathrm{D_s} \to \tau \bar{\nu}_\tau$. The uncertainty on $\mathrm{BR}(\mathrm{b} \to \mathrm{D_s}) = (18 \pm 5)\%$ [22] gave an uncertainty on $\mathrm{BR}(\mathrm{b} \to \tau \bar{\nu}_\tau \mathrm{X})$ of $\pm 0.037\%$. Changing $\mathrm{BR}(\mathrm{D_s} \to \tau\nu) = (7 \pm 4)\%$ [22] by one standard deviation gave an uncertainty of $\pm 0.068\%$.

The spectrum of the missing energy $\mathrm{E_{miss}}$ in $\mathrm{b\overline{b}}$ events depends on the mean energy of the decaying b-hadrons. Changing the mean value $\langle x_\mathrm{b} \rangle = 0.702 \pm 0.008$ [23] by $\pm 1\sigma$ in the simulation and repeating the analysis gave a systematic uncertainty of $\pm 0.21\%$. Similarly the uncertainty from $\langle x_\mathrm{c} \rangle = 0.484 \pm 0.008$ [23] was $\pm 0.03\%$.

Finally, the sensitivity of this measurement to the calibration of the shape of the missing energy distribution of the background events with a sample of events enriched in Z decays into light quark pairs was evaluated as follows. Different energy correction procedures were used with additional terms in (10) like $c_j E_j^2$ and $c_j \sqrt{E_j}$ (with $E_j = E_\mathrm{ch}$, E_γ, E_oth, E_HCAL); the value of χ^2 in (11) was evaluated for different numbers of moments (n=3,4,5); and both moments and central moments were used. These changes gave a maximum change of 0.25% in the branching fraction, and this was taken as the systematic uncertainty. Varying the missing energy range chosen for the fit by ± 5 GeV gave an additional contribution of $\pm 0.15\%$.

All these systematic uncertainties combined in quadrature give a total of $\pm 0.39\%$. Other uncertainties that were considered (for instance on the tau polarization) were found to have much smaller effects. Thus the final result was

$$\mathrm{BR}(\mathrm{b} \to \tau \bar{\nu}_\tau \mathrm{X}) = (2.19 \pm 0.24\ (\mathrm{stat}) \pm 0.39\ (\mathrm{syst}))\% \tag{12}$$

6 Constraints on Type II Higgs models

No indication of an enhancement of the $\mathrm{B^-} \to \tau^- \bar{\nu}_\tau$ branching fraction was observed with respect to the Standard Model prediction ($\mathrm{BR^{SM}}$). In the Type II Higgs models, the branching fraction $\mathrm{BR}(\mathrm{B^-} \to \tau^- \bar{\nu}_\tau)$ is enhanced by a factor of $\left[\left(\frac{m_{\mathrm{B^-}}}{m_{\mathrm{H^\pm}}}\right)^2 \tan^2\beta - 1\right]^2$ [21]. With $m_{\mathrm{B^-}} = 5279$ MeV/c^2 [22] and $\mathrm{BR^{SM}} = 6 \times 10^{-5}$, the limit obtained from (9) is

$$\frac{\tan\beta}{M_{\mathrm{H^\pm}}} < 0.46\ (\mathrm{GeV}/c^2)^{-1} \tag{13}$$

at 90% confidence level. If B_c decays contribute [7], the branching fraction is modified to $BR^{SM}(B_u + B_c) = \alpha \cdot BR^{SM}(B_u)$, where α is a factor ranging from 1.24 to 2.2 which takes into account the $B_c \to \tau\bar{\nu}_\tau$ contribution. If α is 1.24, the previous limit becomes $\frac{\tan\beta}{M_{H^\pm}} < 0.42\ (\mathrm{GeV}/c^2)^{-1}$ at 90% confidence level.

No indication of an enhancement of the branching fraction of $b \to \tau\bar{\nu}_\tau X$ was found with respect to the Standard Model prediction. Using HQET with one loop QCD corrections [21], (12) translates to a limit at 90% confidence level on the charged Higgs mass in the framework of Type II Higgs doublet model:

$$\frac{\tan\beta}{M_{H^\pm}} < 0.48\ (\mathrm{GeV}/c^2)^{-1} \tag{14}$$

7 Summary and conclusion

No signal for the purely leptonic decay $B^- \to \tau^-\bar{\nu}_\tau$ was found in 3.5 million hadronic Z decays at LEP1 in 1992-1995. This gives the upper limit

$$BR(B^- \to \tau^-\bar{\nu}_\tau) < 1.1 \times 10^{-3} \text{ at } 90\% \text{ C.L.}$$

This limit is consistent with the Standard Model expectation $BR^{SM} \simeq 6 \times 10^{-5}$. The branching fraction of $B^- \to \tau^-\bar{\nu}_\tau$ is expected to be significantly larger in models with two Higgs doublets. This limits Type II Higgs doublet model:

$$\frac{\tan\beta}{M_{H^\pm}} < 0.46\ (\mathrm{GeV}/c^2)^{-1} \text{ at } 90\% \text{ C.L.}$$

The possible B_c contribution makes the limit stronger.

The branching fraction

$$BR(b \to \tau\bar{\nu}_\tau X) = (2.19 \pm 0.24\ (\mathrm{stat}) \pm 0.39\ (\mathrm{syst}))\%$$

was obtained from the observed missing energy distribution in a sample enriched in $b\bar{b}$ events but depleted in their semileptonic decays. This value agrees with the Standard Model prediction of $(2.30 \pm 0.25)\%$ [8] and with previous experimental measurements (Figure 6), and gives

$$\frac{\tan\beta}{M_{H^\pm}} < 0.48\ (\mathrm{GeV}/c^2)^{-1} \text{ at } 90\%\text{C.L.}$$

This limit is similar to that deduced from the search for the exclusive channel $B^- \to \tau^-\bar{\nu}_\tau$ but is not influenced by the large uncertainty on $f_B|V_{ub}|$. The upper limits from both analyses are shown in Figure 7, together with the measurements of $b \to s\gamma$ [25]. The direct search for charged Higgs bosons at LEP gives the constraint $M_{H^\pm} > 78.6\ \mathrm{GeV}/c^2$ [26].

Acknowledgments

We thank Y. Grossman of Stanford Linear Accelerator Center, for helping us to calculate the upper limit on $\tan\beta/M_{\mathrm{H}^\pm}$ and S. Slabospitsky of Protvino for useful discussions on B_c contamination.
We are greatly indebted to our technical collaborators, to the members of the CERN-SL Division for the excellent performance of the LEP collider, and to the funding agencies for their support in building and operating the DELPHI detector.
We acknowledge in particular the support of
Austrian Federal Ministry of Science and Traffics, GZ 616.364/2-III/2a/98,
FNRS–FWO, Belgium,
FINEP, CNPq, CAPES, FUJB and FAPERJ, Brazil,
Czech Ministry of Industry and Trade, GA CR 202/96/0450 and GA AVCR A1010521,
Danish Natural Research Council,
Commission of the European Communities (DG XII),
Direction des Sciences de la Matière, CEA, France,
Bundesministerium für Bildung, Wissenschaft, Forschung und Technologie, Germany,
General Secretariat for Research and Technology, Greece,
National Science Foundation (NWO) and Foundation for Research on Matter (FOM), The Netherlands,
Norwegian Research Council,
State Committee for Scientific Research, Poland, 2P03B06015, 2P03B1116 and SPUB/P03/178/98,
JNICT–Junta Nacional de Investigação Científica e Tecnológica, Portugal,
Vedecka grantova agentura MS SR, Slovakia, Nr. 95/5195/134,
Ministry of Science and Technology of the Republic of Slovenia,
CICYT, Spain, AEN96–1661 and AEN96-1681,
The Swedish Natural Science Research Council,
Particle Physics and Astronomy Research Council, UK,
Department of Energy, USA, DE–FG02–94ER40817.

References

[1] J. Alexander *et al.*, CLEO Collaboration, Phys. Rev. Lett. **77** (1996) 5000.

[2] W.-S. Hou, Phys. Rev. **D48** (1993) 2342.

[3] T. E. Browder *et al.*, CLEO Collaboration, "A Search for BR(B$\to \tau\nu$)", hep-ex/0007057, submitted to Phys. Rev. Lett.

[4] R. Barate *et al.*, ALEPH Collaboration, "Measurement of BR(b$\to \tau^-\bar{\nu}_\tau$X) and BR(b$\to \tau^-\bar{\nu}_\tau$D$^{*\pm}$X) and Upper Limits on BR(b$\to \tau^-\bar{\nu}_\tau$) and BR(b$\to$ s$\nu\bar{\nu}$)", hep-ex/0010022, preprint CERN-EP/2000-126 (29 Sept 2000), submitted to Eur. Phys. Journal.

[5] M. Acciarri *et al.*, L3 Collaboration, Phys. Lett. **B396** (1997) 327.

[6] F. Abe *et al.*, CDF Collaboration, Phys. Rev. Lett. **81** (1998) 2432.

[7] M.L. Mangano and S.R. Slabospitsky, Phys. Lett. **B410** (1997) 299.

[8] A. Falk, Z. Ligeti, M. Neubert, Y. Nir, Phys. Lett. **B326** (1994) 145;
A. Czarnecki, M.Jezabek, J.H. Kuhn, Phys. Lett. **B346** (1995) 335.

[9] P. Heiliger and L.M. Seghal, Phys. Lett. **B229** (1989) 409.

[10] B. Grzadkowski and W.-S. Hou, Phys. Lett. **B283** (1992) 427.

[11] G. Isidori, Phys. Lett. **B298** (1993) 409.

[12] M. Acciarri *et al.*, L3 Collaboration, Phys. Lett. **B332** (1994) 201.

[13] OPAL Collaboration, "Measurement of the Branching Ratios b $\to \tau^-\bar{\nu}_\tau$X and b $\to$ D$^{*+}\tau^-\bar{\nu}_\tau$(X)", submitted to the 1996 Warsaw ICHEP Conference, pa05-038.

[14] P. Aarnio *et al.*, DELPHI Collaboration, Nucl. Instrum. and Methods **A303** (1991) 233.

[15] P. Abreu *et al.*, DELPHI Collaboration, Nucl. Instrum. and Methods **A378** (1996) 57.

[16] T. Sjöstrand, Comput. Phys. Commun. **82** (1994) 74.

[17] C. Peterson *et al.*, Phys. Rev. **D27** (1983) 105.

[18] P. Abreu *et al.*, DELPHI Collaboration, Z. Phys. **C66** (1995) 323.

[19] S. Brandt *et al.*, Phys. Lett. **12** (1964) 57.

[20] V.F. Obraztsov, Nucl. Instrum. and Methods **A316** (1992) 388;
V.F. Obraztsov, Nucl. Instrum. and Methods **A399** (1997) 500.

[21] Y. Grossman, H.E. Haber and Y. Nir, Phys. Lett. **B357** (1995) 630;
Y. Grossman and Z. Ligeti, Phys. Lett. **B332** (1994) 373.

[22] Review of Particle Physics, Eur. Phys. J. **C15** (2000) 1.

[23] The LEP Heavy Flavour Working Group, "Input Parameters for the LEP/SLD Electroweak Heavy Flavour Results for Summer 1998 Conferences", LEPHF/98-01, http://www.cern.ch/LEPEWWG/heavy/lephf9801.ps.gz .

[24] P. Abreu *et al.*, DELPHI Collaboration, Eur. Phys. J. **C12** (2000) 209.

[25] M.S. Alam *et al.*, CLEO Collaboration, Phys. Rev. Lett. **74** (1995) 2885;
R. Barate *et al.*, ALEPH Collaboration, Phys. Lett. **B429** (1998) 169.

[26] The LEP working group for Higgs boson searches, "Searches for Higgs bosons: Preliminary combined results using LEP data collected at energies up to 202 GeV", preprint CERN-EP/2000-055 (25 April 2000).

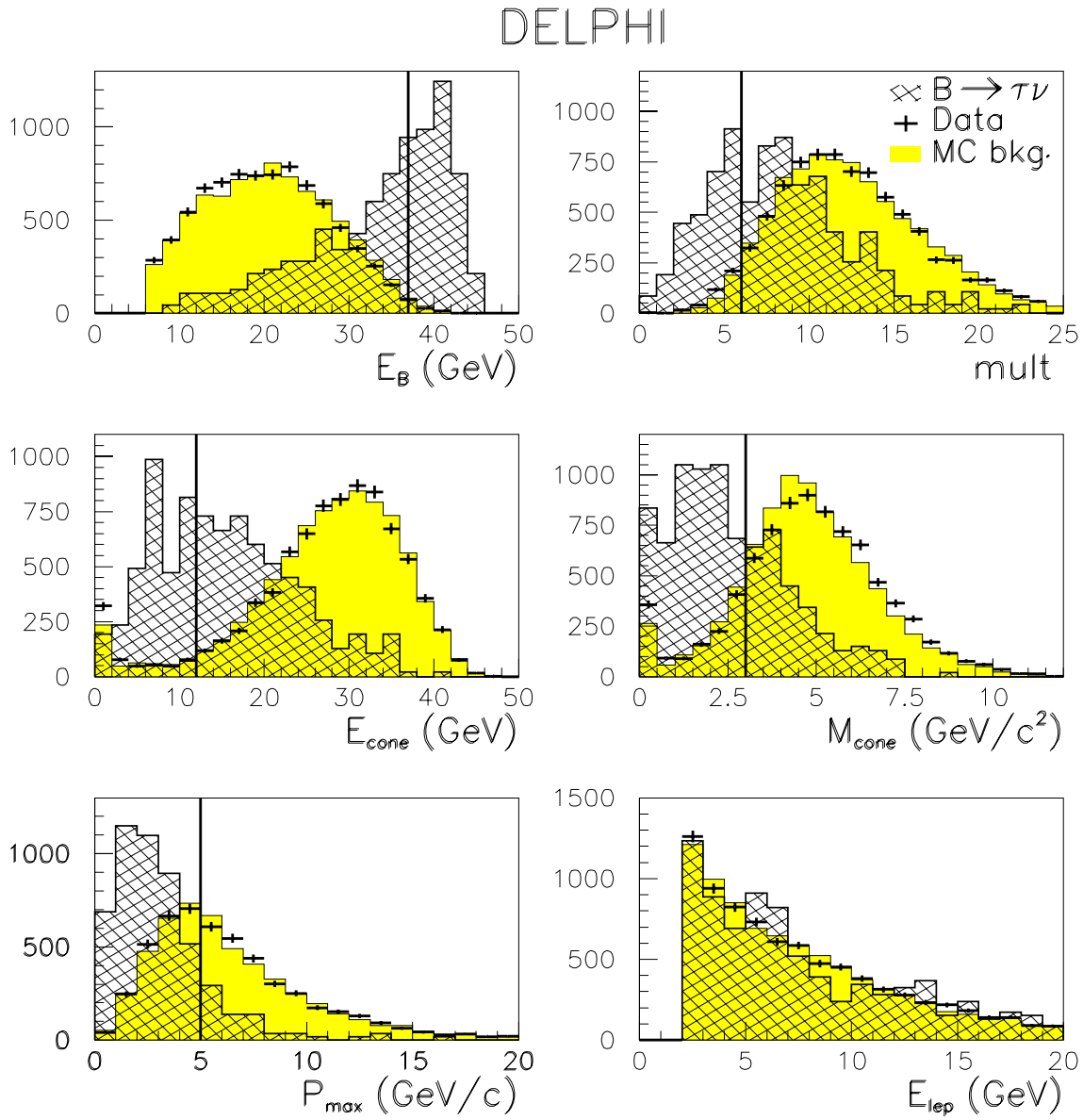

Figure 1: For the leptonic decay channel of the τ, simulated $B^- \to \tau^- \bar{\nu}_\tau$ signal (hatched) and background (shaded) distributions of the fitted B meson energy, the hemisphere charged particle multiplicity, the total energy and invariant mass of the particles inside a 0.5 radian half-angle cone around the lepton, the maximum momentum of particles from the primary interaction, and the lepton energy (see Section 4.1). The crosses show the measured distributions, with simulation normalized to the same integrated luminosity. Distributions for signal events are normalized arbitrarily to the same number of events in the histogram. The vertical lines show the values of the cuts (see Section 4.1).

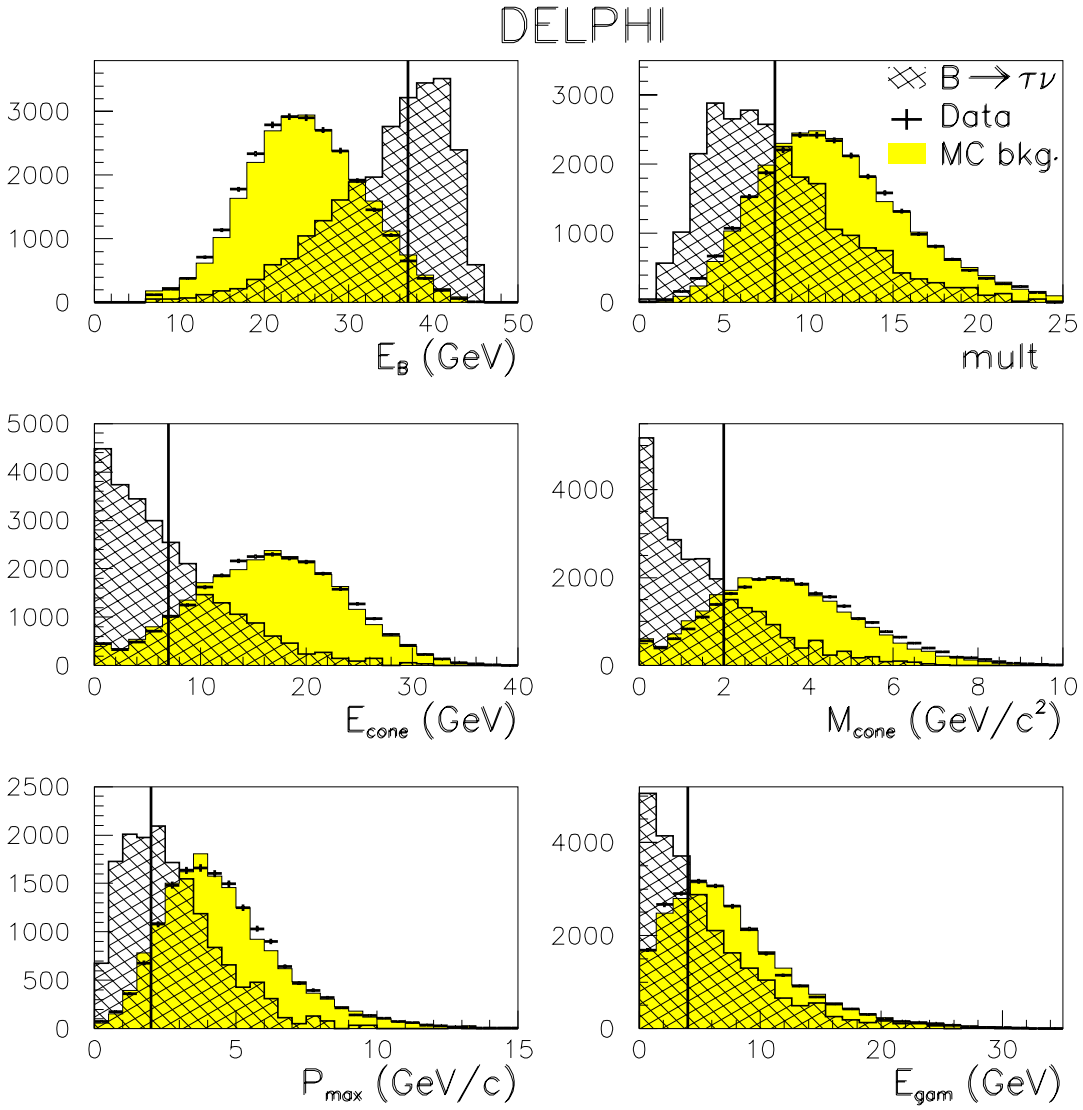

Figure 2: For the hadronic decay channel of the τ, simulated $B^- \to \tau^- \bar{\nu}_\tau$ signal (hatched) and background (shaded) distributions of the fitted B meson energy, the hemisphere charged particle multiplicity, the total energy and invariant mass of the particles inside a 0.5 radian half-angle cone around the charged hadron taken as the candidate τ decay product, the maximum momentum of particles from the primary interaction, and the electromagnetic energy in the cone (see Section 4.2). The crosses show the measured distributions, with simulation normalized to the same integrated luminosity. Distributions for signal events are normalized arbitrarily to the same number of events in the histogram. The vertical lines show the values of the cuts (see Section 4.2).

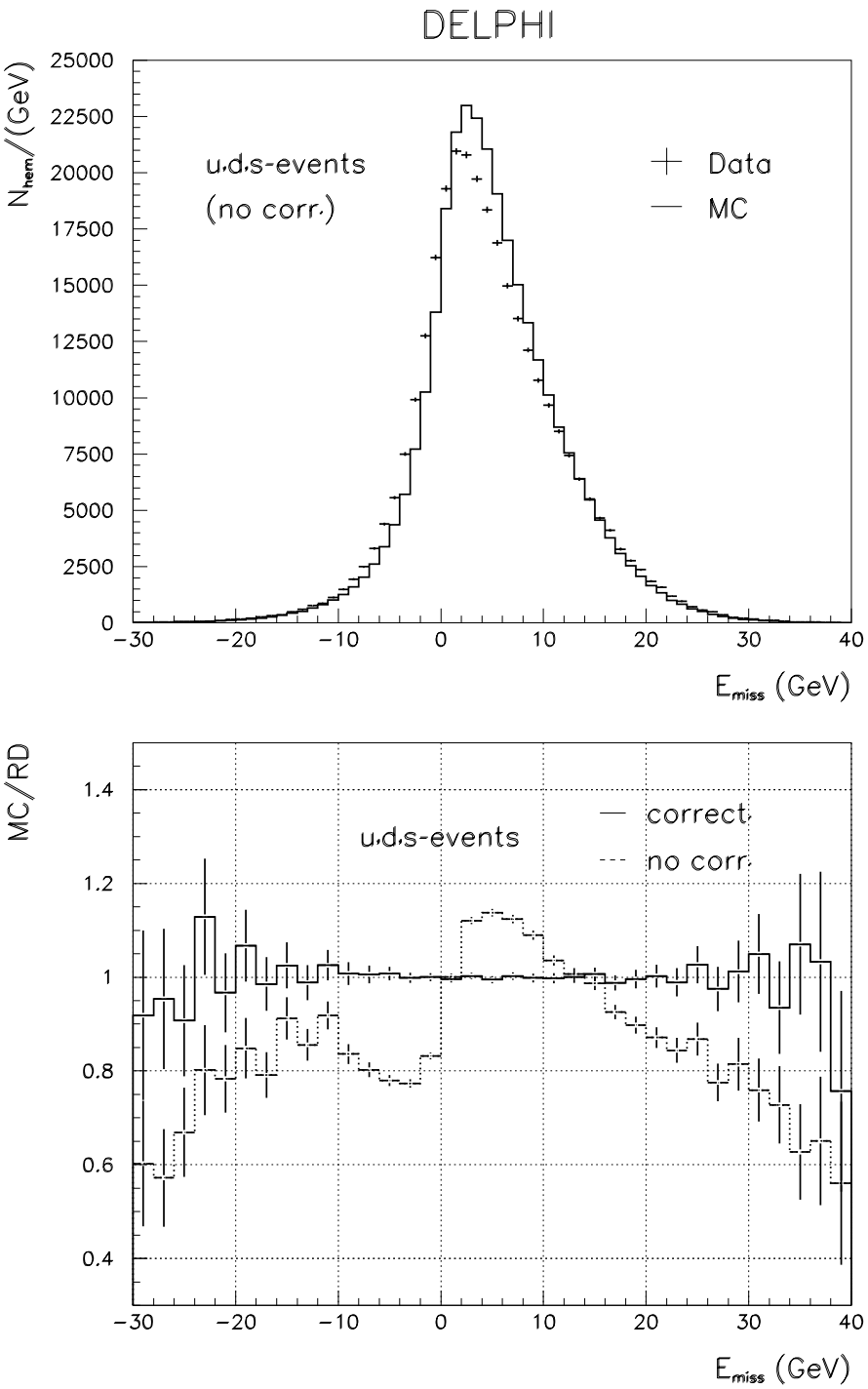

Figure 3: Comparison between real and simulated data of the missing energy distribution in each event hemisphere. The upper plots give these distributions for event samples depleted in heavy flavour decays. The lower plots show the ratio of simulated to real data both before and after the corrections detailed in Section 5.1.

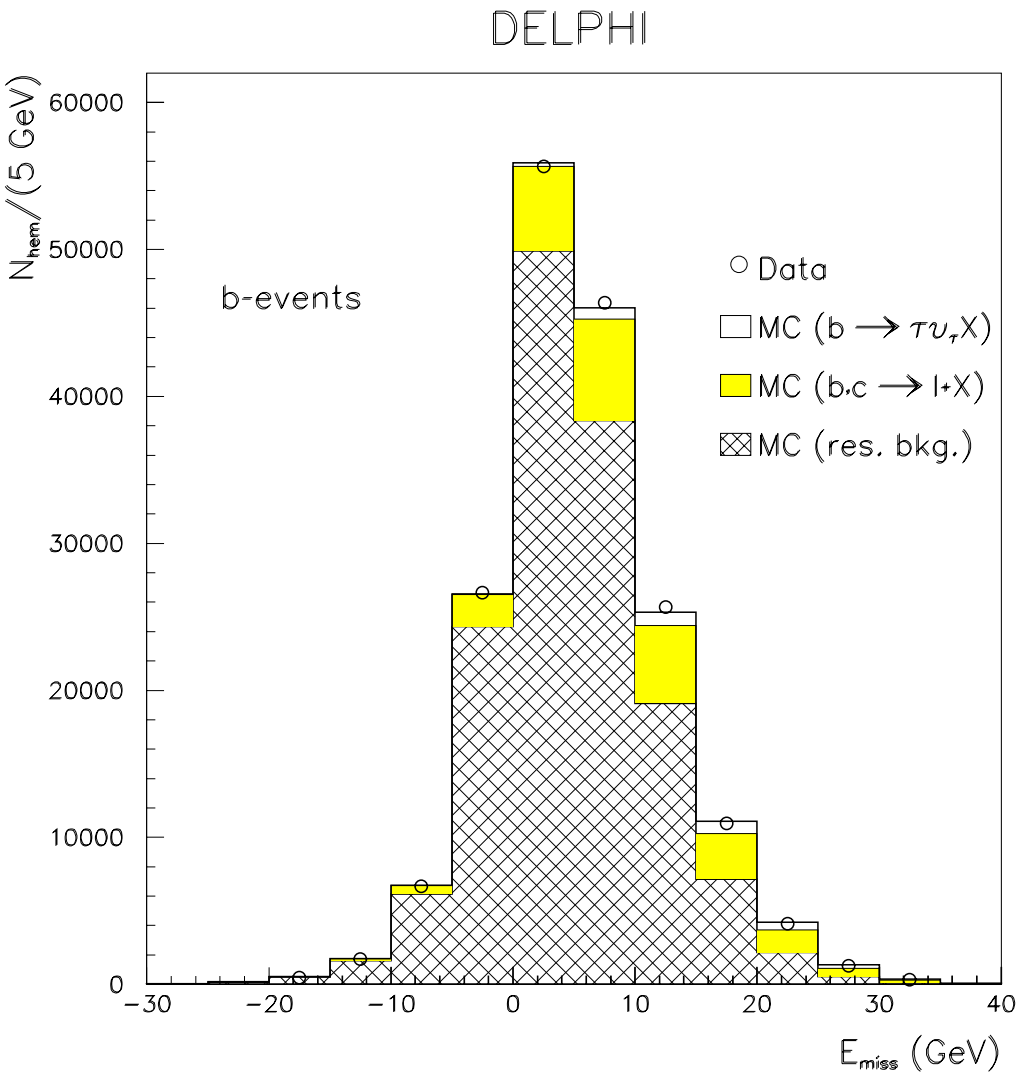

Figure 4: Hemisphere missing energy distributions for real data (circles) and simulation (histograms). The Monte Carlo events are subdivided into the simulated $b \to \tau\bar{\nu}_\tau X$ signal, the semileptonic background, and the residual background.

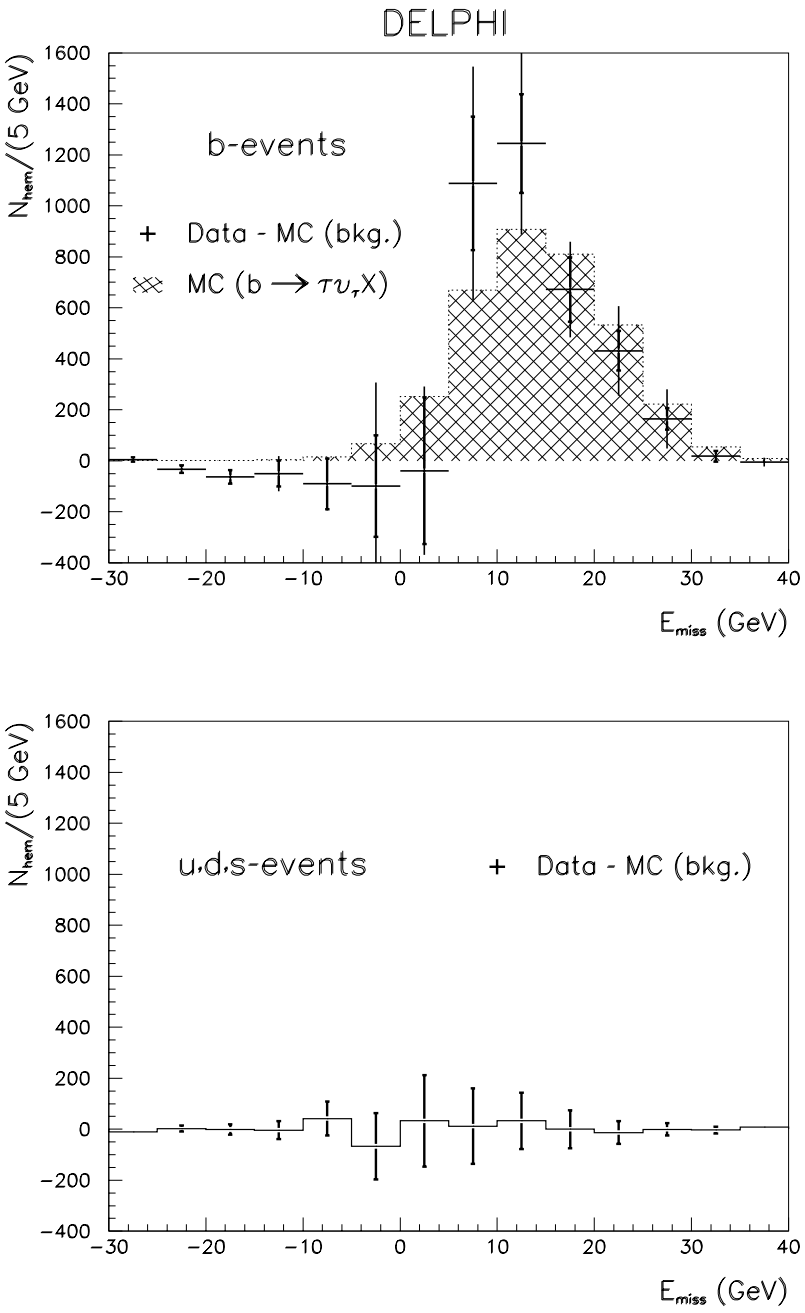

Figure 5: Difference of hemisphere missing energy distributions between real data and background simulation for both b enriched and light-quark (uds) enriched samples. The clear excess of data in the b enriched sample is compared with the predicted missing energy spectrum of the b $\to \tau\bar{\nu}_\tau$X signal (hatched area). The total error bars of the upper plot are computed from the quadratic sum of the statistical and systematic uncertainties. The statistical uncertainties of the data are presented by the thick error bars. The data and Monte Carlo histograms are normalized to the same number of entries in the missing energy range from -5 to 30 GeV.

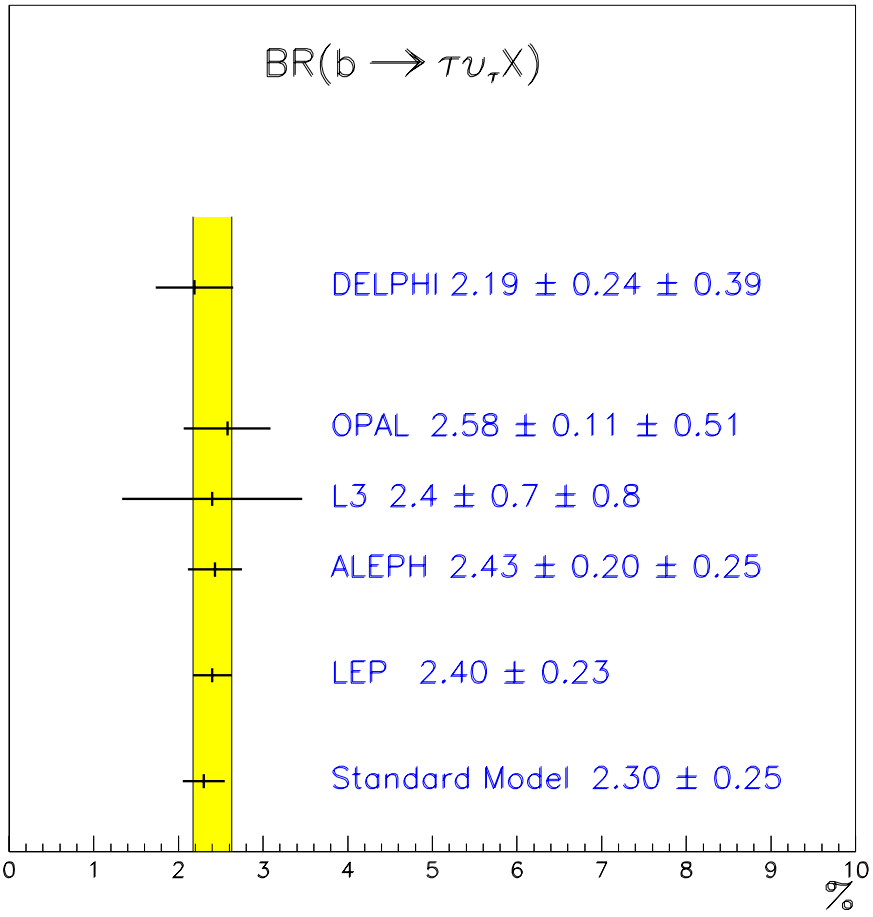

Figure 6: Comparison between the Standard Model prediction and experimental measurements of the b $\to \tau\bar{\nu}_\tau$X branching fraction. All numbers are given in (%).

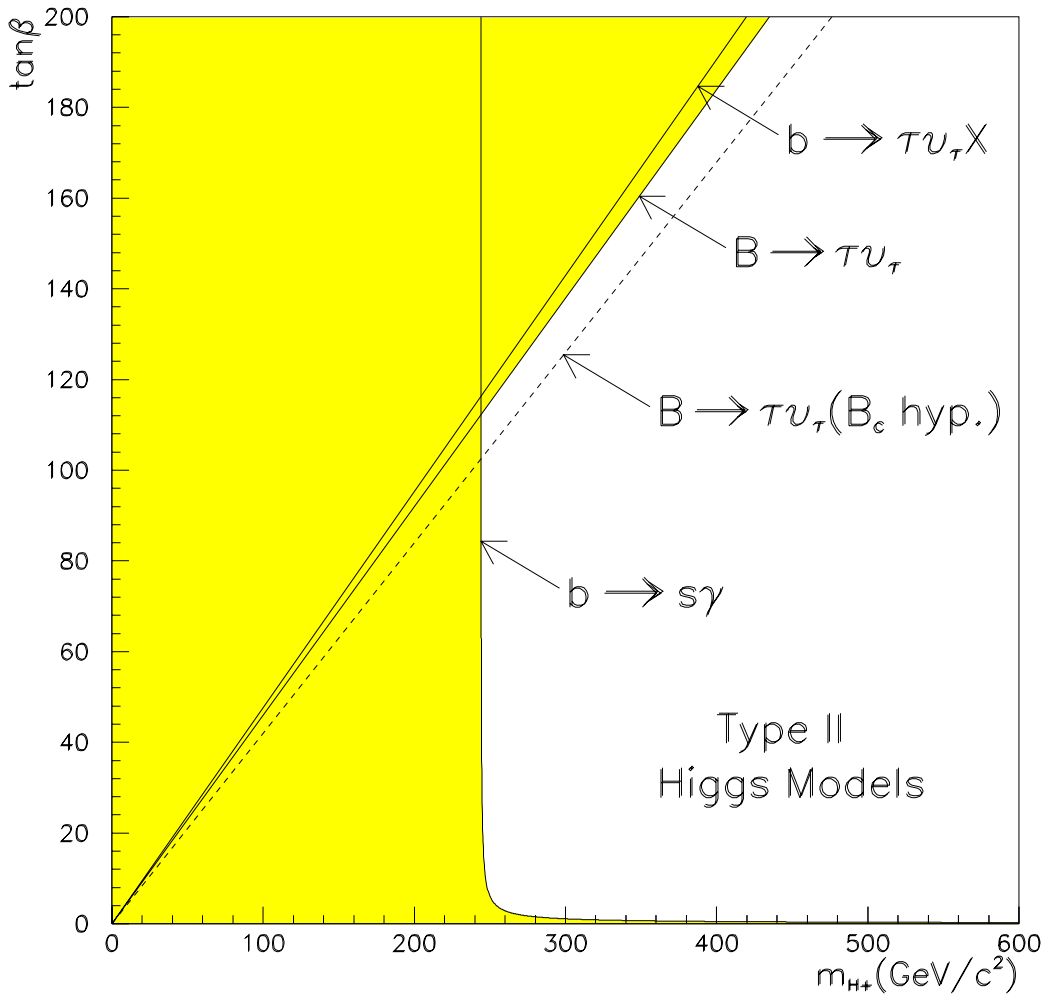

Figure 7: Limits on parameters of Type II Higgs doublet models extracted from the results of the inclusive $b \to \tau \bar{\nu}_\tau X$ and exclusive $B^- \to \tau^- \bar{\nu}_\tau$ analyses, together with the measurements of $b \to s\gamma$ [25]. The dotted line shows the improved limit after including the B_c [7]. Shaded regions are excluded at the 90% confidence level.